*Acta Cryst.* (1955). 8, 43

# The Structure of $FeAl_3$. I

By P. J. Black*

*Crystallographic Laboratory, Cavendish Laboratory, Cambridge, England*

(*Received* 21 *July* 1954 *and in revised form* 1 *November* 1954)

This intermetallic compound has a monoclinic structure, space group $C2/m$, with 100 atoms per unit cell and 42 atomic parameters. The analysis was first performed by a special application of Patterson sections. A projection of the primitive unit cell was used for refinement which gave all the parameters in one two-dimensional synthesis. The process of refinement and the accuracy of the parameters are considered, but discussion of the results is deferred to a subsequent paper.

## 1. Introduction

In this paper, the analysis of the structure of an aluminium–iron compound is described. It is intended to limit the account almost entirely to a discussion of the special techniques used in the solution and refinement of the structure. Other details are available in a thesis (Black, 1954). A discussion of the results, and of metallurgical work on the phase and its transformations, is deferred to a later paper. This phase is usually called '$FeAl_3$' and this name will be retained, although a rather more accurate formula is $Fe_4Al_{13}$.

The first crystallographic measurements on the phase were made by Groth (1906–19), who described the crystals as monoclinic, prismatic in form and twinned. X-ray measurements have been made by Osawa (1933), Bachmetew (1943, 1944) and Phragmén (1950), using single-crystal photographs. They all found the cell to be orthorhombic, with the parameters shown in Table 1.

## 2. Collection of data

### (i) *Symmetry and cell dimensions*

Crystals extracted from an alloy which had been quenched from above 600° C. were used in this work; chemical analysis by Messrs Johnson Matthey and Co. Ltd shows that they contain between 38·5 and 39% iron by weight. They occur as needles with irregular re-entrant faces, as plates and with a prismatic form. The latter are illustrated by Bachmetew (1944). The density of the crystals, determined by a flotation method, is $3{\cdot}77 \pm 0{\cdot}04$ g.cm.$^{-3}$.

Oscillation and Laue photographs showed that the crystals have Laue symmetry $2/m$, with pseudo-orthorhombic symmetry. Weissenberg photographs, taken with crystals oscillating about the twofold axis, show that they are twinned and that the twinning accentuates the pseudo-symmetry. The diffraction spots could be separated into two lattices, with a constant intensity ratio between their corresponding spots, and with their orientations related by a reflexion. This ratio was different for each crystal and some crystals showed more complicated multiples. Attempts to produce a single crystal by cutting, grinding and etching of crystals were not successful. The unit cell is monoclinic, with a $C$-face centring and Laue symmetry $2/m$. Accurate parameters were measured by adapting the method of Farquhar & Lipson (1946) to the monoclinic symmetry. The final values are given in Table 1. The measurements of previous workers are consistent with these results if the confusion about the symmetry is attributed to the twinning.

### (ii) *The intensity data*

These were recorded with a twinned crystal of linear dimensions 0·15 mm. ($\fallingdotseq 1/\mu$ for Mo $K\alpha$ radiation) and approximately cubic form. For each exposure, a multiple-film technique was used. Intensities were measured by visual comparison with a standard scale. Photographs for the layers $h0l$ to $h7l$ and $hk0$ were collected and measured, using filtered molybdenum radiation.

For reflexions of the types $0k0$ and $hkn$ (where $n$ is a multiple of 8) the different reflexions from the two components of the twinned crystal superpose. A set of twin-related spots was measured to determine

Table 1. *Unit-cell dimensions of* $FeAl_3$

| | Symmetry | $a$ (Å) | $b$ (Å) | $c$ (Å) |
|---|---|---|---|---|
| Osawa (1933) | Orthorhombic | 15·804 | 8·088 | 11·870 |
| Bachmetew (1944) | Orthorhombic | 15·49 | 8·11 | 47·6 |
| Phragmén (1950) | Orthorhombic | 15·59 | 8·10 | 48·04 |
| Present work | Monoclinic | $15{\cdot}489 \pm 0{\cdot}001$ | $8{\cdot}0831 \pm 0{\cdot}0005$<br>$\beta = 107° 43' \pm 1'$ | $12{\cdot}476 \pm 0{\cdot}002$ |
| | | ($a:b:c = 1{\cdot}5435:1:1{\cdot}9155$) | | |
| Groth (1906–19) | Monoclinic | ($a:b:c = 1{\cdot}5413:1:1{\cdot}9158$; $\beta = 107° 41'$) | | |

---

* Royal Society Mr and Mrs John Jaffe Donation Student.

the ratio of the two components, and from this ratio corrections could be calculated for the superposed spots. This correction was checked by comparing the results with similar readings from a crystal where the ratio of the two components had a much larger value. The agreement was well within the limit expected for eye-estimated intensities. Corrections were applied for Lorentz and polarization factors (Cochran, 1948) and for absorption, using the corrections derived by Bradley (1935) for a cylindrical specimen.

### (iii) *The space group*

From the Laue symmetry and systematic absences, space groups $C2/m$, $Cm$, $C2$ are possible. The measured intensities were first used to determine the space group by statistical methods. Distribution curves for the $(h0l)$, $(hk0)$ and $(hkl)$ intensities were drawn (Howells, Phillips & Rogers, 1950). The first of these indicated that the $(h0l)$ zone is centrosymmetrical, which means that there is a twofold axis. The second was inconclusive—it was later seen that in this projection the scattering material is mainly located in four large peaks. The third showed that the space group must be centrosymmetrical. As a final check, the mean intensity for the reciprocal-lattice layers perpendicular to the $b$ axis was obtained; the ratio of the mean $(h0l)$ intensity to the mean intensity for $(h1l)$ to $(h7l)$ was 1·83, indicating the presence of a mirror plane. These tests therefore strongly favour the space group $C^3_{2h}$–$C2/m$.

## 3. Solution of the structure

(i) The mean composition, determined from the chemical analysis, corresponds to 23·4 atomic% iron. The number of atoms of each kind was calculated using this result and the measured density and cell volume. The numbers so obtained were 23·4 iron atoms and 76·6 aluminium atoms per unit cell. In using these figures it had to be remembered that they might be in error owing to inaccuracy in the determination of the density and to variable composition, or that they might correspond to a larger number of sites not all of which are fully occupied. General positions in this space group have an eightfold multiplicity.

(ii) The first analysis was based on the $(0k0)$ reflexions. These indicate that the atoms lie in four well defined layers perpendicular to the $b$ axis. Two of these must lie on the mirror planes at $y = 0$ and $y = \frac{1}{2}$, which are related by the $C$ centring. The layer between them can be puckered. Examination of the $(hk0)$ Patterson projection, and attempts to correlate the $(0k0)$ intensities with calculated values, showed that most of the atoms in this puckered layer are at heights $y = 0{\cdot}215$ and $0{\cdot}285$ and that the majority of the weight is in the flat layer, in the ratio 1·25:1. At this stage, therefore, it was known that just over half the atoms are on mirror planes (fourfold positions) and the rest between these planes (eightfold positions). The asymmetric unit would then contain about eighteen atoms, six between the planes and twelve on them.

(iii) The first main feature of interest in this analysis is the adaptation of Patterson methods to the special conditions of this problem, namely the prominent layers and their relation to the symmetry elements.

The combination of mirror plane and $C$-face centring produces an $a$-glide plane at height $y = \frac{1}{4}$ and perpendicular to $b$, by which atoms at $y = 0{\cdot}215$ are related to those at $y = 0{\cdot}285$. To investigate the $x$–$z$ parameters, three portions of the three-dimensional Patterson were constructed. The first was a section at $y = 0$ which would show the vectors between atoms in the flat layer and between atoms at the same height in the puckered layer. The second was a slab (section-projection) between $y = 0{\cdot}215$ and $y = 0{\cdot}285$, which would show vectors between atoms in the flat layer and those in the puckered layer. The third was a section at height $y = 0{\cdot}07$ to show vectors between atoms at the different heights in the puckered layer. Data up to and including $k = 7$ were required to prevent serious overlap between these sections (Bragg & West, 1930).

Of these three syntheses the third contains the smallest number of vectors and the following analysis was applied (Fig. 1($a$)). Atom $A$ is repeated by the $a$-glide plane at $B$. A third atom, $C$, at the same height as $A$, produces a vector peak $C$–$B$ at height $y = 0{\cdot}07$ and a peak $C$–$A$ at height zero. Fig. 1($b$) shows the section at $y = 0{\cdot}07$, and it can be seen that the $C$–$B$ peak from the true origin, is the same as a $C$–$A$ peak referred to an origin at $O'$ distance $a/2$ along $x$. If all atoms in the puckered layer lie at the two heights 0·215 and 0·285, then the section at 0·07 referred to this new origin is the section at height zero for the atoms in the puckered layer only. This could be subtracted from the section at height zero, and the

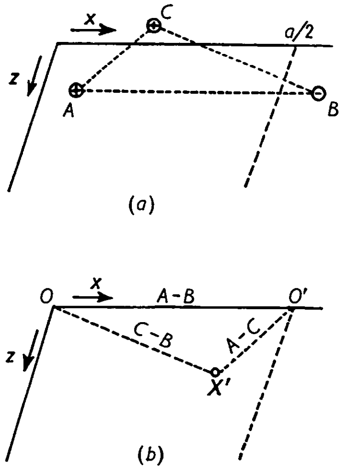

Fig. 1. The atomic pattern ($a$) and the derived Patterson ($b$) for a pair of atoms in the puckered layer.

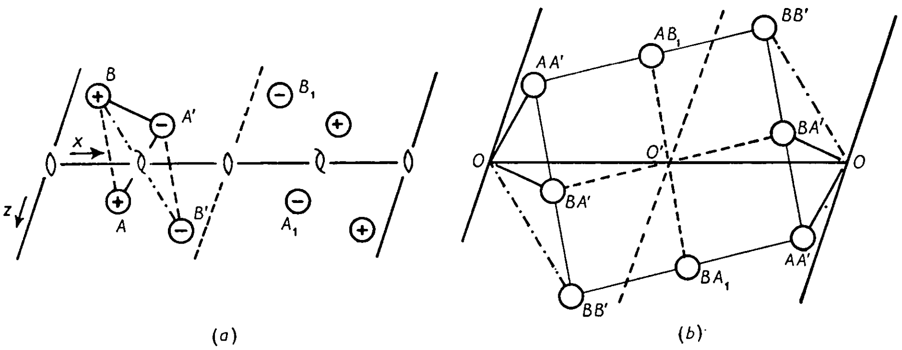

Fig. 2. Development of Fig. 1 for all atoms related by symmetry to two unrelated atoms. Atomic pattern (*a*) and Patterson (*b*).

difference would be a Patterson section for vectors between atoms in the flat layer only. The analysis could be further developed to show that any two atoms in the puckered layer give eight related peaks in its Patterson, and this is presented in Fig. 2.

An examination of the peaks around the origins ($O$ and $O'$) of the section at $y = 0{\cdot}07$ showed that around $O$ there is a set of peaks at 2·4 Å (Fe–Al distance) whilst around $O'$ there are no peaks closer than 2·7 Å (Al–Al distance). The peaks around $O$ could be split into two pentagons which are centrosymmetrically related, with the peaks of each pentagon about 2·8 Å from each other. It was deduced that an iron atom at $y = 0{\cdot}285$ is surrounded by a pentagon of aluminium atoms at $y = 0{\cdot}215$. Various ways of arranging this unit were tried so that, under the symmetry operations, it would pack with its neighbours, and the only successful one gave the pattern of Fig. 3, with extra atoms placed on the twofold axis. The Patterson of this arrangement was checked with the observed Patterson section, and was in good agreement if some allowance was made for overlap effects from the peaks at $y = 0$.

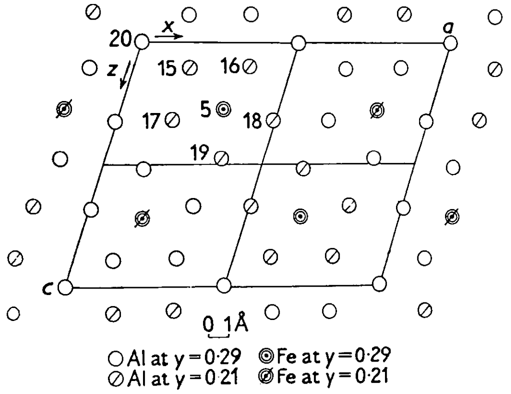

Fig. 3. The first pattern for the atoms in the layer puckered about $y = 0{\cdot}25$.

(iv) The flat layer at $y = 0$ is sandwiched between the puckered layer and its mirror image; this so limits the space available that packing considerations determined the pattern of this layer. The result is shown in Fig. 4. For this again, a check was made with the Patterson sections, and moderately good agreement was obtained.

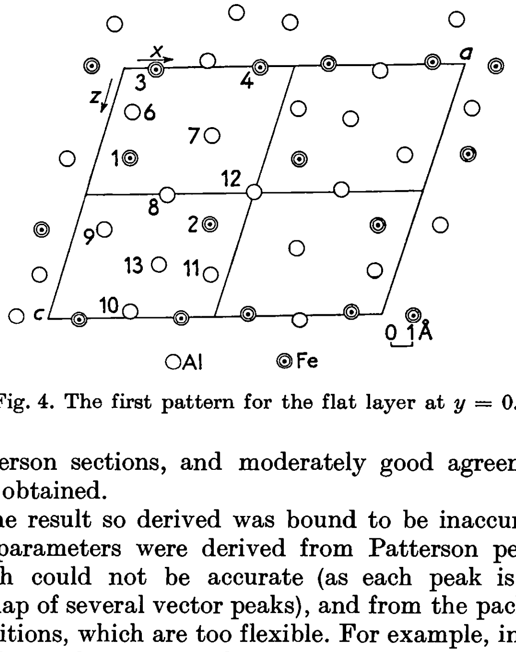

Fig. 4. The first pattern for the flat layer at $y = 0$.

The result so derived was bound to be inaccurate. All parameters were derived from Patterson peaks, which could not be accurate (as each peak is the overlap of several vector peaks), and from the packing conditions, which are too flexible. For example, in the flat layer there are twelve atoms in the asymmetric unit (only one of which is on a special position) to be adjusted to each other and to atoms in the puckered layer, which each have three variable parameters. Neither was the number of atoms certain. For example, it was doubtful whether the sites marked 7 and 13 (Fig. 4) would actually be occupied as they are very near to other atoms.

## 4. Refinement of the structure

(i) The first attempts at refinement were made by using one- and two-dimensional Fourier syntheses. Although the agreement of observed and calculated structure factors was improved by this method, accurate parameters could not be obtained because of the superpositions of atoms in all three axial projections. It was also thought that false minima might be obtained with the large number of variable parameters if only a small number of $F$'s was employed.

(ii) The second main feature of this analysis is the use of a primitive projection in the centred lattice to obtain three-dimensional parameters. The need for this sort of device arose because the alternative at this stage was the use of three dimensional data, for which higher-layer Weissenbergs are not very accurate and whose collection on oscillation photographs would be tedious on account of the ambiguity arising from the large cell and the twinning. The primitive (triclinic) cell is shown in Fig. 5(*a*); two axial projections of this are the same as for the original cell, but the third, down $b'$, is quite different.

The new cell has a volume of one-half of the old cell. It is easily seen that in its ($h0l$) zone of reflexions there are no systematic absences, so that the asymmetric unit of the $b'$ projection is twice the size of the asymmetric unit of the monoclinic $b$ projection. The transformation of co-ordinates is easily calculated (Fig. 5(*b*)). The $z$ co-ordinates remain unchanged. If $x_m, y_m$ are the fractional co-ordinates on the monoclinic axes and $x_t$ similarly the triclinic co-ordinate, then it can be shown that

$$x_t = x_m - y_m \, .$$

For atoms on the mirror plane, $y_m = 0$. An atom in the puckered layer at $x_m, y_m, z_m$ is repeated by the $a$ glide plane at $x_m + \frac{1}{2}, \frac{1}{2} - y_m, z_m$. If the triclinic parameters of these are distinguished by $t_1$ and $t_2$ respectively, it follows that

$$\begin{aligned} x_m &= \tfrac{1}{2}(x_{t2} + x_{t1}) \, , \\ y_m &= \tfrac{1}{2}(x_{t2} - x_{t1}) \, , \\ z_m &= z_{t1} = z_{t2} \, . \end{aligned}$$

All three co-ordinates are obtained because atoms related by symmetry in the monoclinic cell appear twice in the triclinic projection as independent peaks.

Refinement on this projection has two other advantages. First, all the measured data were collected on one zero-layer Weissenberg photograph. Secondly, a plan of atomic positions in projection (see Fig. 6) shows that most of them are clearly resolved, and, where they are not, the resolution is simplified as one atom is fixed on a line (atom 20) or on a symmetry centre (atom 12).

The main disadvantage is that all three-dimensional parameters are adjustable variables in the projection, the number of terms concerned in structure factor calculations is very large, and the number of observed reflexions is also very large.

(iii) A first calculation of the first 100 (low-angle) structure factors for this zone gave an $R$ factor of 0·41, which was high compared with the agreement on the previous projections ($R = 0{\cdot}23$) and emphasizes their limitations for determining three-dimensional parameters. The first refinements were made by calculating successive $F_o$ syntheses on low-angle reflexions ($\sin\theta/\lambda < 0{\cdot}35 \times 10^8$ cm.$^{-1}$). The refinement was slow and irregular. The $R$ factor was reduced to 0·31 and then the method was abandoned in favour of ($F_o - F_c$) syntheses.

(iv) The problem at this stage was the refinement of a projection with 42 parameters and 420 $F$'s, where the inclusion of one or two doubtful atoms made very little difference to the overall agreement, and where the atomic positions had originally been in error by as much as 0·7 Å, and were still between 0·1 and 0·3 Å from their final positions. It was hoped that the use of ($F_o - F_c$) syntheses would avoid the dangers of false minima which were encountered with the work on $F_o$ syntheses, and would permit refinement with the minimum of calculation. These hopes were justified by the following procedure.

A limited number of $F$'s ($\sin\theta/\lambda < 0{\cdot}21 \times 10^8$ cm.$^{-1}$) were used in the first syntheses, and these were refined from $R = 0{\cdot}32$ to 0·17. Then further sets of data were introduced in stages, and refined by ($F_o - F_c$)'s until $R$ was below 0·20 at the end of each stage. After eleven ($F_o - F_c$)'s, all data with $\sin\theta/\lambda < 0{\cdot}55 \times 10^8$ cm.$^{-1}$ had been included. Then all strong reflexions at higher angles were included, and the remaining weaker ones were introduced at successive stages. After twenty ($F_o - F_c$)'s, the $R$ factor on all reflexions was reduced to 0·17. (In this, for unobserved reflexions, the amount by which $F_c$ came above the limit of observation was reckoned as error). A review of those rows which had been corrected for superposition due to twinning

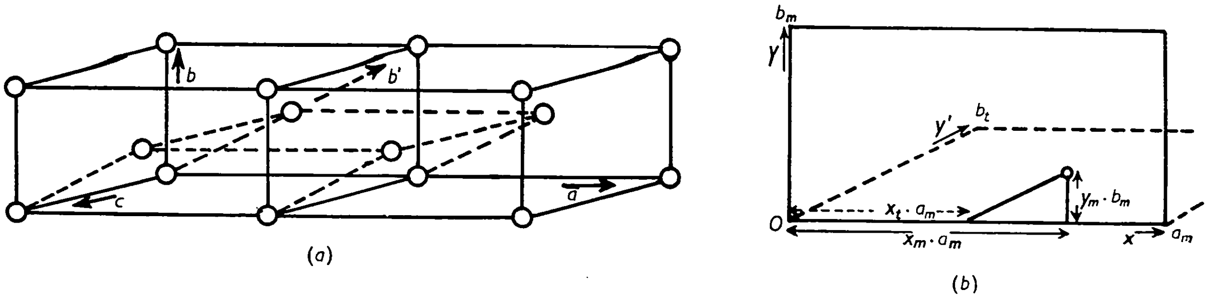

Fig. 5. (*a*) Monoclinic (full line) and triclinic (broken line) cells. Two monoclinic cells are shown. The $a$ and $c$ axes of the two types coincide.

(*b*) Relationship between parameters of monoclinic and triclinic projections.

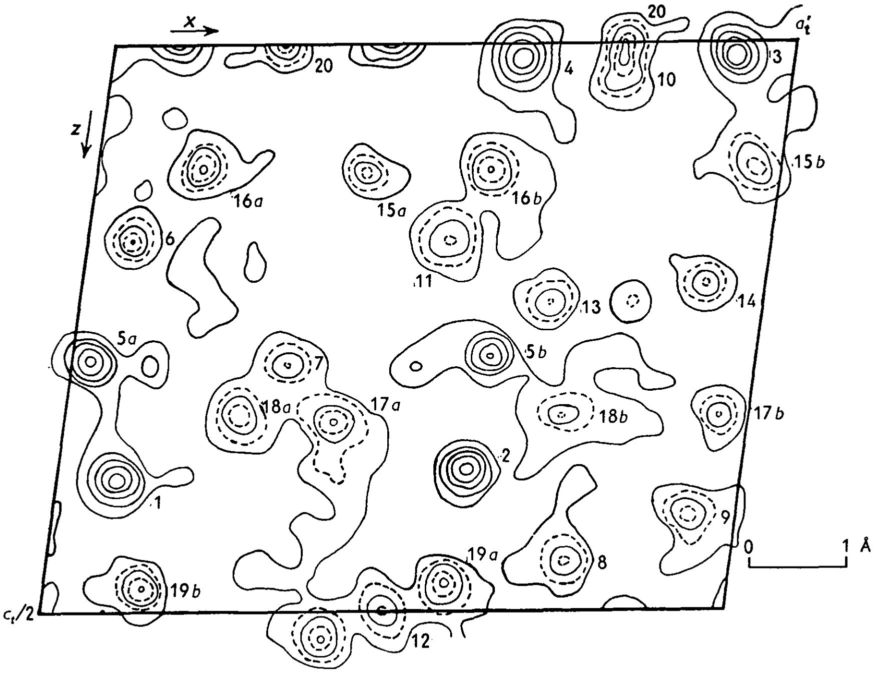

Fig. 6. The $(h0l)_t$ Fourier projection of the asymmetric unit of the triclinic $b$-axis projection. $a_t'$ is the length of $a_t$ shortened by projection on to a plane normal to $b_t$; $c_t$ lies in this plane. Different positions of the same atom are indicated by $a$ and $b$ suffixes. Positive contours at equal intervals are shown by full lines, intermediate contours by broken lines. There is no $F(000)$ term in the synthesis.

showed that a 5% change in the twinning ratio used for this correction gave a considerable improvement in the correlation of observed and calculated $F$'s, and the change was adopted as it lies within the range of uncertainty of the original determination of the ratio. A full list of observed and calculated $F$'s is available elsewhere (Black, 1954).

(v) A final $F_o$ synthesis is shown in Fig. 6. Five weak reflexions, comprising 0·1% of the total weight $(\Sigma F_o)$ are omitted because their calculated value is too small to assign their signs. There are many spurious features which are due to overlap effects and do not appear on $(F_o - F_c)$ syntheses. An $F_c$ synthesis was calculated, and termination corrections were applied using the method due to Booth (1946). All parameters were determined by fitting the peaks to parabolas. The final $F_o$ synthesis was calculated at 3° intervals, giving an interval of 0·13 Å along $x$ and 0·10 Å along $z$. In all $F_c$ calculations Fermi–Thomas scattering factors were used. The temperature factor used is discussed in the next section. The final parameters are listed in Table 2. There are 24 iron and 78 aluminium atom sites in the cell; the final syntheses show that one aluminium site (no. 7) is only 70% occupied.

(vi) Throughout the refinement, calculated $(F_c)$ values were scaled to the observed $(F_o)$ values in the usual way. The variation of the scaling factor $(G)$ was analysed. At high angles, a graph of log $G$ against $\sin^2\theta/\lambda^2$ is a straight line from which the temperature factor was found. After correction for the effect of this at low angles, the residual variation was mainly accounted for by the effect of progressive resolution of the $\alpha$ doublet on eye-estimated intensity. Nothing could be deduced about the other possible effects, namely extinction and errors in the $f$ curves for $F_c$. For the final synthesis the $F_o$'s were all scaled to the $F_c$'s and then multiplied by the (natural) temperature factor.

Table 2. *Atomic parameters in* $FeAl_3$
(Monoclinic axes)

| Atom | No. in cell | $x$ | $y$ | $z$ |
|---|---|---|---|---|
| Fe 1 | 4 | $0{\cdot}086_5$ | 0 | $0{\cdot}383_1$ |
| Fe 2 | 4 | $0{\cdot}401_8$ | 0 | $0{\cdot}624_3$ |
| Fe 3 | 4 | $0{\cdot}090_7$ | 0 | $0{\cdot}989_0$ |
| Fe 4 | 4 | $0{\cdot}400_1$ | 0 | $0{\cdot}985_7$ |
| Fe 5 | 8 | $0{\cdot}318_8$ | $0{\cdot}285_0$ | $0{\cdot}277_0$ |
| Al 6 | 4 | $0{\cdot}064_5$ | 0 | $0{\cdot}173_0$ |
| Al 7 | $4\times0{\cdot}7$ | $0{\cdot}322_3$ | 0 | $0{\cdot}277_8$ |
| Al 8 | 4 | $0{\cdot}235_2$ | 0 | $0{\cdot}539_2$ |
| Al 9 | 4 | $0{\cdot}081_2$ | 0 | $0{\cdot}582_4$ |
| Al 10 | 4 | $0{\cdot}231_7$ | 0 | $0{\cdot}972_9$ |
| Al 11 | 4 | $0{\cdot}480_3$ | 0 | $0{\cdot}827_7$ |
| Al 12 | 2 | $\frac{1}{2}$ | 0 | $\frac{1}{2}$ |
| Al 13 | 4 | $0{\cdot}310_0$ | 0 | $0{\cdot}769_5$ |
| Al 14 | 4 | $0{\cdot}086_9$ | 0 | $0{\cdot}781_2$ |
| Al 15 | 8 | $0{\cdot}188_3$ | $0{\cdot}216_4$ | $0{\cdot}111_1$ |
| Al 16 | 8 | $0{\cdot}373_4$ | $0{\cdot}211_0$ | $0{\cdot}107_1$ |
| Al 17 | 8 | $0{\cdot}176_5$ | $0{\cdot}216_8$ | $0{\cdot}334_3$ |
| Al 18 | 8 | $0{\cdot}495_9$ | $0{\cdot}283_2$ | $0{\cdot}329_6$ |
| Al 19 | 8 | $0{\cdot}366_4$ | $0{\cdot}223_8$ | $0{\cdot}479_9$ |
| Al 20 | 4 | 0 | $0{\cdot}244_1$ | 0 |

## 5. The accuracy of the structure

The value of $\sigma(F_o)$ calculated from the mean of $(F_o-F_c)$ was 6·0 (Cochran, 1951), which is an overestimate. Two independent sets of readings of the same zone from the same crystal gave $R = 5{\cdot}6\%$, and for the same row from two different crystals gave $R = 8{\cdot}2\%$. The latter value corresponds to $\sigma(F_o) = 2{\cdot}8$. A value of 4·5 was used for a safe estimate of $\sigma(F_o)$. The parameter $p$, defined by the equation

$$\varrho(r) = \varrho(0)\exp(-pr^2)\,,$$

was found from the final $F_o$ synthesis. The results for iron and aluminium were 18·4 and 17·2 respectively. The peaks are much sharper here than in the work of Cochran (1951) and Penfold (1952), where values of $p$ between 4 and 5 are recorded. The results obtained for $\sigma(x_r)$, using Booth's (1947) equation, were:

$$\text{Fe: } \sigma(x_r) = 0{\cdot}002\ \text{Å}, \quad \text{Al: } \sigma(x_r) = 0{\cdot}005\ \text{Å};$$

and, using Booth & Britten's equation (1948), were:

$$\text{Fe: } \sigma(x_r) = 0{\cdot}006\ \text{Å}, \quad \text{Al: } \sigma(x_r) = 0{\cdot}013\ \text{Å}\,.$$

The mean values of these two were used. For atoms on the mirror plane, $y = 0$ and the $x$ and $z$ (monoclinic) parameters have deviations $\sigma$. For atoms not at $y = 0$, $z$ co-ordinates are derived directly from the triclinic projection, and there are two readings for each atom: the standard deviation between these pairs of parameters should be $\sqrt{2}.\sigma = 0{\cdot}011$ Å. The mean value actually found was 0·009 Å. Each $x$ and $y$ (monoclinic) parameter is calculated from a pair of parameters and so has a standard deviation $\sqrt{2}.\sigma$. The standard deviation of an interatomic distance then depends on the position ($y = 0$ or $y \neq 0$) and character (iron or aluminium) of the pair of atoms concerned; the values range from 0·006 Å to 0·02 Å—most of them are about 0·013 Å.

$\sigma(\varrho_o)$ from the formulae of Lipson & Cochran (1953) has values of 3·3 and 1·5 e.Å$^{-2}$ respectively, so that a reasonable estimate is 2·5 e.Å$^{-2}$. The standard deviation in the number of electrons counted in an area of 1 Å$^2$, using the formula of Cochran (1951), is 0·6 electrons.

## 6. Conclusions

The Patterson analysis used to obtain the approximate structure in this problem is not of direct general application, but it does show that, where prominent layers are found, Patterson sections parallel to them may be of special value.

The use of a primitive cell to aid refinement in a centred lattice gave a quite unexpected and powerful result; its application to other space groups will be considered elsewhere. It can be appreciated that in this work the device saved a great deal of labour, and methods which help the process of refinement in this way will become more important as the analysis of complex structures is extended through the development of direct methods.

This same consideration applies to the third feature, the problem of refinement in § 4(iv). It is felt that the procedure outlined there is the most efficient strategy for this type of problem; it can be contrasted with the more laborious and less rewarding use of $F_o$ syntheses in § 4(iii).

I wish to thank Prof. G. V. Raynor and Dr A. R. Harding for their help in providing specimens. I am indebted to Prof. Sir Lawrence Bragg and Dr W. H. Taylor for provision of facilities and for their interest in the progress of this work. I am particularly grateful to Dr Keith Robinson for constant advice and encouragement. I thank the Department of Scientific and Industrial Research and the Council of the Royal Society for financial support.

## References

Bachmetew, A. (1943). *Z. Kristallogr.* **88**, 179.
Bachmetew, A. (1944). *Z. Kristallogr.* **89**, 575.
Black, P. J. (1954). Dissertation for Ph.D. degree, Cambridge.
Booth, A. D. (1946). *Proc. Roy. Soc.* A, **188**, 77.
Booth, A. D. (1947). *Proc. Roy. Soc.* A, **190**, 482.
Booth, A. D. & Britten, K. H. V. (1948). *Proc. Roy. Soc.* A, **193**, 305.
Bradley, A. J. (1935). *Proc. Phys. Soc.* **47**, 879.
Bragg, W. L. & West, J. (1930). *Phil. Mag.* **10**, 823.
Cochran, W. (1948). *J. Sci. Instrum.* **25**, 253.
Cochran, W. (1951). *Acta Cryst.* **4**, 81.
Farquhar, M. C. M. & Lipson, H. (1946). *Proc. Phys. Soc.* **58**, 200.
Groth, P. (1906–19). *Chemische Krystallographie*, vol. 1. Leipzig: Engelmann.
Howells, E. R., Phillips, D. C. & Rogers, D. (1950). *Acta Cryst.* **3**, 210.
Lipson, H. & Cochran, W. (1953). *The Determination of Crystal Structures*. London: Bell.
Osawa, A. (1933). *Sci. Rep. Tôhoku Univ.* **22**, 803.
Penfold, B. R. (1952). Dissertation for Ph.D. degree, Cambridge.
Phragmén, G. (1950). *J. Inst. Met.* **77**, 489.